



Synergistic co-processing of an acidic hardwood derived pyrolysis bio-oil with alkaline Red Mud bauxite mining waste as a sacrificial upgrading catalyst



Elham Karimi^a, Ivo Freitas Teixeira^{a,b}, Ariel Gomez^c, Eliane de Resende^{a,d}, Christopher Gissane^a, Jay Leitch^a, Véronique Jollet^a, Isabella Aigner^e, Franco Berruti^e, Cedric Briens^e, Peter Fransham^f, Brent Hoff^g, Nick Schrier^g, Rochel M. Lago^b, Stefan W. Kycia^c, Richard Heck^h, Marcel Schlaf^{a,*}

^a Department of Chemistry, The Guelph-Waterloo Centre for Graduate Work in Chemistry (GWC)², University of Guelph, Guelph, Ontario, N1G 2W1, Canada

^b Departamento de Química, Universidade Federal de Minas Gerais, Belo Horizonte Brasil, MG 31270-901, Brazil

^c Department of Physics, The Guelph-Waterloo Physics Institute (GWPI), University of Guelph, Guelph, Ontario, N1G 2W1, Canada

^d Universidade Federal de Lavras – UFLA, Lavras, MG, 37200-000, Brazil

^e Institute for Chemicals and Fuels from Alternative Resources (ICFAR), The University of Western Ontario, 22312 Wonderland Rd. North RR#3, London, Ontario, N0M 2A0, Canada

^f ABRI-TECH Inc., Namur, Quebec, Canada

^g Laboratory Services Division, University of Guelph, Guelph, Ontario, N1G 2W1, Canada

^h Department of Land Resource Science, University of Guelph, Guelph, Ontario, N1G 2W1, Canada

ARTICLE INFO

Article history:

Received 21 November 2012

Received in revised form 30 January 2013

Accepted 2 February 2013

Available online 11 February 2013

Keywords:

Biomass conversion

Pyrolysis bio-oil

Bio-fuel

Catalytic upgrading

Bauxite mining waste

Red Mud

ABSTRACT

In this proof-of-concept study we demonstrate that co-processing of an acidic bio-oil ($\text{pH} < 3$) produced by the fast pyrolysis of sawmill residue hardwood chips with alkaline ($\text{pH} > 12$) Red Mud bauxite mining waste originating from the Bayer process can lead to a synergistic upgrading and value addition to both feed materials. The co-processing reaction is carried out in a pressure reactor at 365°C and yields a stabilized, much less acidic and more energy-dense bio-oil with an oxygen content of 3.5% and heating value of 34 kJ/g compared to 43.1% and 12 kJ/g, respectively, for the crude oil. In the same reaction the Red Mud acts as a sacrificial catalyst and is converted into a partially reduced magnetic neutral gray material with a carbon content of $\sim 33\%$ (w/w). This neutralized material may have possible use as an iron ore, iron ore pelletization binder or soil additive. The co-processing of the two waste streams – one derived from forestry by-products, the other from bauxite mining and processing operations – may thus offer attractive economic and ecologic synergies. Two principle possible scenarios for an actual realization for such a process on a larger scale are discussed.

© 2013 Elsevier B.V. All rights reserved.

1. Introduction

The fast pyrolysis of ligno-cellulosic biomass to bio-oil holds substantial promise for the development of a large scale renewable fuel supply decoupled from the production of food [1–4]. The advantages of the pyrolysis route for the conversion of biomass into fuel lie in its conceptual simplicity, universal applicability to practically any type of plant derived biomass, a high degree of energy densification by almost an order of magnitude compared to the raw biomass and the fact that a pumpable and (within limits) storable liquid product is obtained.

Challenges arise from the fact that the fast pyrolysis process generates bio-oil as a highly reactive and complex non-equilibrium mixture of several hundred compounds containing water, carboxylic acids (notably formic and acetic acid), (hydroxy-)ketones, (hydroxy-)aldehydes, alkenes, alcohols, furans, phenols and others [5,6], that is intrinsically unstable to secondary acid catalyzed aldol condensations, esterifications, etherifications, oligomerizations and polymerizations within the bio-oil. This typically leads to resin formation and phase separation of an aqueous layer as the oil ages or if purification/fractionation by vacuum distillation is attempted. The high oxygen ($\sim 40\%$), water (20–25%) and acid content (up to 10% of carboxylic acids) and consequently low pH (~ 2) of the oil also limit its direct use as a fuel due to corrosion and poor or inconsistent burn characteristics. Therefore a catalytic upgrading process that both stabilizes and deoxygenates the bio-oil and converts it into a liquid that can either directly serve as a

* Corresponding author. Tel.: +1 519 824 4120; fax: +1 519 766 1499.

E-mail address: mschlaf@uoguelph.ca (M. Schlaf).

high-energy density fuel or be used as a feedstock in existing petrochemical refineries is typically necessary. The two main approaches to a catalytic upgrading of pyrolysis bio-oil are hydrodeoxygenation (hydrotreating) using a supported hydrogenating metal or cracking using a zeolite or other catalysts. The current state of the intense ongoing research efforts in this area has recently been expertly reviewed by Bulushev and Ross [3], Jensen and co-workers [7] and Bridgwater [4]. Regardless of the approach taken, the aqueous acidic nature and intrinsic high reactivity of the bio-oil pose a major problem and challenge, as rapid catalyst deactivation through fouling or coking or even hydrolytic destruction of the support matrix and leaching of the active hydrogenating metal can occur resulting in either short catalyst lifetime or at least the need to continuously regenerate the catalyst. Both scenarios add major capital and/or operating costs. It can thus be argued that the development of effective and robust catalyst systems adapted to the specific requirements of bio-oil upgrading constitutes one of the main hurdles for its wide-spread development as a renewable fuel in an economically viable manner [8].

A very inexpensive and therefore potentially *sacrificial* catalyst system that could possibly answer to this challenge is Red Mud bauxite mining waste [9]. Red Mud is produced at ~120 megatons/year and stored either as a slurry in lagoons or as a sludge in *dry-stacking* storage sites that to date amount to an estimated total of 3 gigatons of deposited material worldwide [10]. As the byproduct of the Bayer process for the production of pure Al_2O_3 , Red Mud is a mineralogically highly complex mixture of iron, aluminum, silicon and titanium oxides [11–14]. Table 1 summarizes the general composition of Red Mud and lists the mineral phases typically present. Due to its high alkalinity, to date no ecologically and economically satisfactory remediation or recycling processes exist for Red Mud and its storage sites constitute a substantial safety and environmental hazard [15–18].

Under reducing conditions at elevated temperature the iron(III) oxides present in the material (mainly hematite and goethite) can be converted to iron(II) oxides (e.g., magnetite, wüstite), iron carbides or even iron metal, all of which can act as Fischer–Tropsch (FT), water-gas-shift-reaction (WGSR) and hydrogenation catalysts for carboxylic acids [19,20]. Recognizing this fact, Red Mud has long been investigated as a catalytically active material for various substrates and reactions, notably for coal and biomass liquefaction and the treatment of bitumen and heavy crude, in which the presence of different phases of TiO_2 , Al_2O_3 and SiO_2 may impart synergistic effects on the overall activity and behaviour of the catalyst that are not well understood, but can nevertheless exploited on an empirical basis [21–31]. We recently demonstrated the use of Red Mud as a catalyst for the effective conversion of formic and acetic as well as levulinic acid to non-acidic deoxygenated products and also successfully used it as an upgrading catalyst on an unusual low-acidity hemp-seed derived bio-oil under high-pressure hydrogen atmosphere [32–34]. Here we report a first example of the application of this material to the upgrading of an acidic hardwood chip derived bio-oil produced in a commercial operation that is more representative of a typical bio-oil and provide a detailed comparative before/after analysis of both the oil and the catalyst that suggests that a co-processing of pyrolysis bio-oil with Red Mud, i.e., the combination waste streams from agri- and silviculture with that of aluminum mining may offer ecologically and economically attractive synergies.

2. Experimental

2.1. General

An authentic operational sample of Red Mud was supplied by Rio Tinto Alcan's Jonquière, Quebec operation [35]. GC analysis was

performed on a Varian 3800 GC using a 30 m DB-1701 column operating at a constant flow rate of 1 mL/min. GC–MS analysis were performed either on a Varian Saturn 2000 GC–MS running in default EI mode (4 V axial bias, 1400 V multiplier) or at the Advanced Analysis Centre of the University of Guelph. GC–MS fragmentation patterns of unknowns were matched to NIST 2005 and/or Saturn databases supplied with the instruments. Gas samples from the headspace of the reactor were qualitatively analyzed using an SRI 8610 micro-GC fitted with a TCD with the retention times calibrated against authentic samples of the linear C_1 – C_6 alkanes and C_2 – C_6 terminal alkenes (1000 ppm in helium; Grace-Davison) as well as CO_2 . Water contents were determined by Karl–Fischer titration using a Metrohm 870 KFTitritino Plus titroprocessor. pH values (relative to starting solutions) were determined by diluting the starting bio-oil as well as the polar and non-polar phases obtained 1:9 with either water (polar/aqueous phase) or methanol (non-polar phase), respectively, and measuring the pH using a Metrohm 827 pH lab glass electrode calibrated against authentic buffer solutions (Metrohm 6.2307.110, pH 7 at 25 °C phosphate based aqueous buffer solution). The pH values cited are thus not directly equivalent to the aqueous scale, but refer to the relative acidities before and after upgrading in their respective methanol sample solutions, i.e., are only meaningful in comparison to each other. A Nicolet 380 FT-IR was used for IR analysis (neat, CaF_2 cells/plates). Heating values were determined using an IKA C 200 bomb calorimeter. Elemental analysis was carried out using a Thermo Fisher (Elantech) FLASH 2000 CHNS/O analyzer. The X-ray powder diffraction (XRD) data were collected on a STOE two circle goniometer using the $\text{Cu K}\alpha$ radiation ($\lambda = 1.54178 \text{ \AA}$) produced by an ENRAF NONIUS FR571 rotating anode X-ray generator. The pattern was measured in the interval from 5 to 60 in 2θ using a 0.02 step size and 40 s of counting time. The transmission Mössbauer spectroscopy experiments were carried out on a spectrometer CMTE model MA250 with a $^{57}\text{Co}/\text{Rh}$ source at room temperature using $\alpha\text{-Fe}^0$ as reference. TGA analyses were carried out in a Shimadzu TGA-60, with a heating rate of 10 °C/min under an air flow of 100 mL/min. The surface areas of the Red Mud before and after use as a catalyst were determined by dinitrogen adsorption (assumed cross-sectional area 16.2 \AA^2) using the BET method in a Quantachrome 4200e instrument. Samples were degassed for 12 h at 30 °C prior to duplicate simultaneous measurements. A standard porous Al_2O_3 sample was also recorded along with each run to ensure consistency between the different samples. The average surface area of the standard was found to be $103.956 \pm 0.13 \text{ m}^2/\text{g}$ for the three sample runs. An empty sample tube was also placed in the Quantachrome 4200e to record the room pressure after every 3 data points as a baseline to minimize the error from pressure changes throughout the run. For the sodium analysis approximately 0.1 g of sample was digested with 3 mL of conc. HCl. Samples were digested at room temperature for 48 h, 2 h at 90 °C, an additional 1 mL of conc. HCl was added and digested at 110 °C for 1 h. The sample was cooled to ambient temperature and brought up to 50 mL final volume with nanopure water. Solutions were filtered and run for sodium by ICP-OES at the University of Guelph Laboratory Services Division (an ISO 9001:2000 registered and SCS/GLP certified facility). A small amount of particulate remained after digestion, i.e., a total digest was not achievable, however due to the generally high solubility of sodium salts this residue was assumed not to contain any sodium. The magnetic susceptibility of samples was determined against a standard sample of 1% Fe_3O_4 in aluminum oxide and epoxy resin using a Bartington MS2 meter equipped with a MS2B Dual Frequency Sensor, capable of taking measurements at both low (χ_{LF} at 0.46 kHz) and high (χ_{HF} at 4.6 kHz) frequencies. The sample of known volume was placed in a polyethylene vial (2.2 cm diameter) and the exact weight measured for the determination of its density (ρ). The volume susceptibility (κ) recorded was converted to the mass specific

Table 1Representative composition of Red Mud bauxite mining waste.^a

Elemental composition	Approximate relative abundance [%]	Actual mineralogy
$\alpha\text{-Fe}_2\text{O}_3$, $\alpha\text{-FeO(OH)}$	41	Hematite Goethite
Al_2O_3	17	Sodalite, Cancrinite, Dawsonite, Tricalcium aluminato, Hydrocalumite, Boehmite Al-substituted $\text{Fe}_x\text{Al}_y\text{O}_z$, Gibbsite, Diaspore
SiO_2	10	Sodalite, Cancranite, Quartz
TiO_2	9	Rutile, Anatase, Perovskite, Ilmenite
CaO	9	Calcite, Perovskite, Whewellite, Tricalcium aluminato, Hydrocalumite
Na_2O	5	Sodalite, Cancranite, Dawsonite
Other (H_2O , trace metals, organic residues, process added flocculants)	10	n/a

^a See Supplementary Material for an actual analysis (by XRF) of the Red Mud supplied by Rio Tinto ALCAN's Jonquière, Quebec operation used in this study.

susceptibility (χ) by $\chi = \kappa/\rho$. Blank readings on an empty vial were taken before and after duplicate readings of each sample to correct for instrument drift.

2.2. Production of pyrolysis bio-oil

ABRI-Tech Inc. operates a 1 dry ton per day dryer/auger pyrolysis system of proprietary configuration at its facility in Namur, Quebec. Hardwood sawdust from the local sawmill was first pulverized and dried to less than 10% moisture in a chain flail type dryer. Dryer operating parameters were adjusted to produce the desired moisture content and a particle size with at least one dimension less than 3 mm. ABRI-Tech's pyrolysis system uses 0.6 mm carbon steel shot as a heat carrier. Since the biomass is quickly incorporated into the hot steel shot carrier, the rate of heat transfer is very rapid ($>1000\text{ }^{\circ}\text{C/s}$). Vapour residence time in the pyrolyzer is estimated at 2 s from evolution to first stage quenching, while the solid residence time of the co-produced bio-char is approximately 5 min. The reactor temperature is maintained at $450 \pm 10\text{ }^{\circ}\text{C}$. The exit temperature of the vapour condensing into the bio-oil is in part a function of the moisture content and is generally 10–20 °C lower than the reaction temperature. The majority (>90%) of the co-produced bio-char is immediately separated from the hot pyrolysis vapours. The presence of the remaining entrained fine char results in the production of a heavy tar phase which phase separates from the acidic lighter water-containing product oil phase used in this study. The ash content of this oil phase was <0.5% (w/w) by ignition.

2.3. Co-processing reactions

All reactions were carried out in a 300 mL Parr reactor (316 SS) fitted with a pressure dial, gold coated burst disc ($p_{\text{max}} = 34.8\text{ MPa}$) and a vent valve. In a typical experiment bio-oil (25 g) and Red Mud (7 g) and – were applicable 25 g of additional water – were mixed in the stainless steel autoclave. As a safety measure in order to displace any air/oxygen the unit was sealed, flushed with hydrogen gas at ambient temperature and pressure, but not pressurized. For a total headspace volume of the reactor of 250 mL and applying the virial gas theorem for hydrogen gas at ambient temperature (298 K) and pressure the total amount of hydrogen introduced into the reactor by this safety measure is <10 mmol, i.e., stoichiometrically insignificant compared to the amounts of substrate and Red Mud used meaning that essentially no external reductant was supplied to the reaction. Reactions were stirred magnetically using a glass coated stir bar and brought to the reaction temperature of 365 °C (measured internally through a 316 SS thermo couple well) at a heating rate of 3 °C/min using an electric band heater. After 4 h at that temperature a gas sample was taken from the headspace of the reactor

and analyzed by micro-GC and GC-MS. The reactor was cooled to ambient temperature, opened and its content (products + catalyst) removed and weighed. From this mixture, bio-oil samples for GC and GC-MS were prepared either by using the phase separated organic phase or, if no organic phase was observed, by separating the aqueous phase from the reaction mixture by decanting and then extracting the residual solid (catalyst with adsorbed organic products) with CHCl_3 and MeOH followed by filtration and removal of the solvent in vacuo (rotavap at $40\text{ }^{\circ}\text{C}/16\text{ Torr}$ for 40 min.). IR spectra were obtained either directly from the separated organic product phase or from the extracted liquid products obtained by the above procedure.

3. Results

3.1. Bio-oil/Red Mud co-processing reactions

Red Mud catalyst and fresh bio-oil (i.e., used within <10 days of its production) were heated to 365 °C in a 316SS pressure reactor and held at that temperature for 4 h with stirring (the heating rate was 3 °C/min. for a total reaction time of ~6 h). This reaction temperature was chosen on the basis of our earlier results, that established ~350 °C as the threshold for the activation of Red Mud as a catalyst by reduction to iron suboxides [33]. Table 2 gives an overview of key properties of the crude bio-oil and upgraded product phases isolated as well as a comparison to the results of control reactions in the absence of Red Mud as a catalyst. The control reactions did not yield any liquid organic product phases, but only an aqueous layer along with a black sticky solid residue that was not further analyzed [36].

Notable are the substantially higher pressures in the reactor in the presence of catalyst at the reaction temperature and after cool-down back to ambient, pointing to a higher amount of gaseous products formed in these reactions. As expected on the basis of our previous results [33,34], qualitative analysis of a gas sample from the headspace of the reactor after the reaction by micro-GC indeed showed substantially higher amounts of the carboxylic acid ketonization side product $\text{CO}_2(\text{g})$ for the reactions with catalyst. Also observed were small amounts of C3–C5 alkenes and alkanes in the gas phase products [37].

The best upgrading result (Entry 3, Table 2) was achieved, when an equal volume of water was added to the reaction mixture, which resulted in a clean phase separation into an acidic aqueous (bottom) and a clear light brown organic product layer (top) that were easily separated from the solid catalyst sedimented at the bottom of the reactor by decanting. Fig. 1 shows the visual appearance of this organic product phase compared to that of the much darker and opaque crude bio-oil with some phase separated water droplets.

Table 2
Upgrading reactions and the properties of bio-oil before and after the reaction.

Description		Pressure		Organic products				Aqueous products				Recovered catalyst	
Entry	Bio oil/reaction	P ₃₆₅ [MPa] ^c	P _{RT} [MPa] ^d	Yield [g]/[% (w/w)] ^e	Water content [%] ^e	pH	TAN ^f	Yield [g]	Water content [%] ^e	pH	TAN ^f	Weight [g]/water content [%] ^e in catalyst residue	Weight increase in re-isolated and dried catalyst, [g]
1	Untreated	n/a	n/a	n/a	37	2.8	123.4	n/a	n/a	n/a	n/a	n/a	n/a
2	Control Reaction with water (no RM catalyst) ^a	15.86	0.69	0 ^g	n/a	n/a	n/a	7.6	84	3.6	67.3	n/a	n/a
3	Reaction with RM catalyst and added water ^a	20.68	2.07	5.9/24 ^h	<1	5.2	19.6	0.5	90	5.2	11.2	9.0/35.9	2.4
4	Control Reaction without water (no RM catalyst) ^b	10.34	0.69	0 ^g	n/a	n/a	n/a	8.8	82	3.2	112.2	n/a	n/a
5	Reaction with RM catalyst without water ^b	12.41	2.07	3.9/16 ⁱ	<1	5.7	2.8	9.4	90	7	0	2.5/15.7	3.4

^a Reaction conditions: bio-oil (25 g), water (25 g) and RM (7 g), 4 h at 365 °C – see also Section 2.

^b Reaction conditions: bio-oil (25 g) and RM (7 g), 4 h at 365 °C – see also Section 2.

^c Maximum pressure recorded at 365 °C.

^d Pressure after cool-down to ambient temperature (22 °C).

^e By Karl-Fischer-titration and excluding added water.

^f 1 g of the organic or aqueous product phase was dissolved in 1 g ¹Pr—OH and 0.5 g water the pH measured with a calibrated electrode the solution titrated with 0.1 M aq. KOH to pH 7 (electrode) and the required amount of KOH [mg] calculated as the total acid number TAN.

^g No liquid organic phase formed – instead a sticky black solid was isolated.

^h 3.7 g clear light brown separated oil phase + 2.2 g oil extracted from catalyst with CHCl₃.

ⁱ Clear light brown oil extracted from catalyst with CHCl₃.



Fig. 1. Appearance of the bio-oil before (left) and after (right, Table 2, entry 3) upgrading using Red Mud as the catalyst.

A similar organic product was obtained in the absence of added water, but required extraction from the residual inorganic solids with chloroform and methanol followed by solvent removal in vacuo, as no defined liquid organic layer remained after decanting the aqueous product phase. The yields of isolated organic products from these reactions were 24 and 16% (w/w with respect to

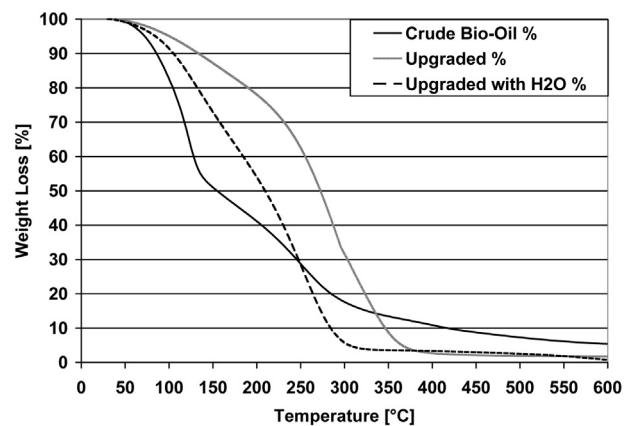


Fig. 3. Comparative TGA analysis of the crude and upgraded (Table 2, entry 3) bio-oil.

bio-oil used), respectively. In order to obtain enough material for the comparative before after analysis described below, the reaction of entry 3, Table 2 was repeated multiple times. The results and yields reported in Table 2 were repeatable within $\pm 10\%$ of the values given.

3.2. Comparative before/after analysis of organic products

A comparative before/after analysis of the bio-oil and the upgraded product was carried by out by variety of techniques.

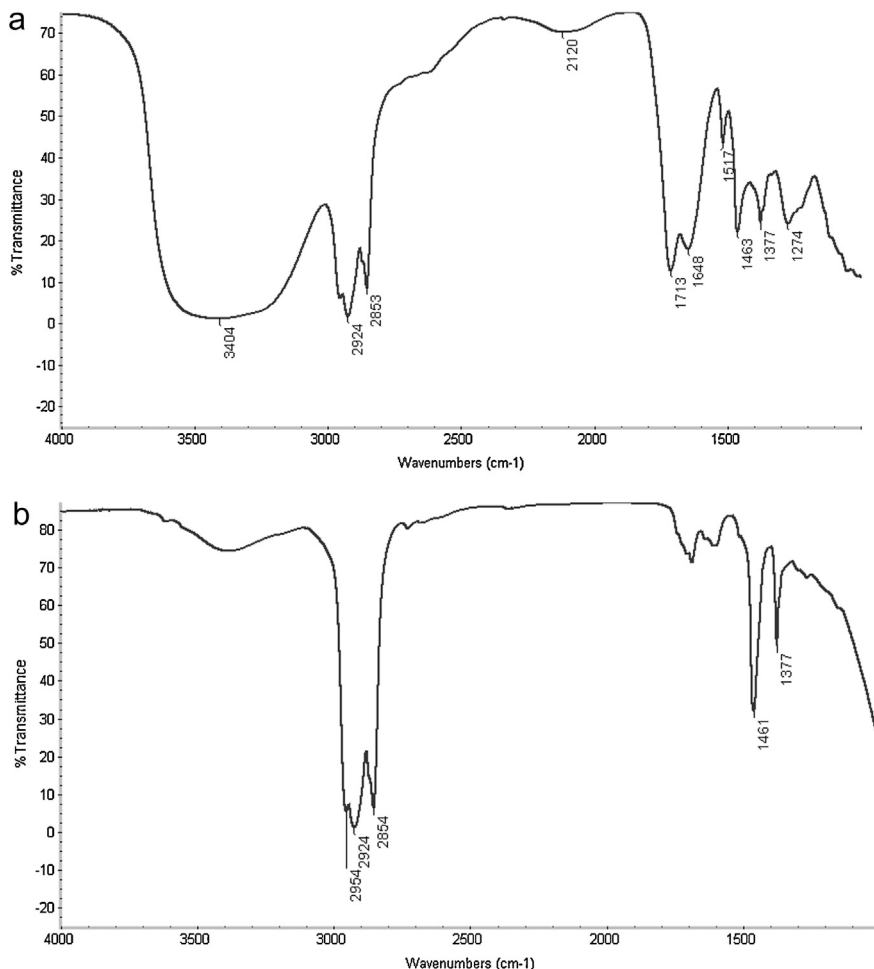


Fig. 2. IR spectra of crude wood bio oil (Top) and the organic product phase of wood bio oil upgraded as described in the text (bottom, Table 2, entry 3) (neat film, CaF_2 cell).

Table 3

Comparative ultimate analysis and heating values of the bio-oil before and after upgrading.

Element	Crude	Upgraded
Carbon [%]	33.4	80.3
Hydrogen [%]	5.3	11.5
Oxygen [%]	43.1	3.5
Nitrogen [%]	0	0.1
Sulfur [%]	0	0
Heating value [kJ/g] ^a	12	34

^a As higher heating values.

Table 2 lists the total acid number (TAN) and water content of the crude and upgraded oil fractions by Karl-Fischer titration. The TAN of the product oils isolated is reduced by at least factor 10 and their total water content <1%, compared to a 37% water content for the crude bio-oil. The polar aqueous phases isolated show a water content of 80–90% and for the Red Mud catalyzed reactions also have a much higher pH and lower TAN than the crude oil. IR spectroscopy (Fig. 2) of the upgraded oil confirms the loss of water (broad peak at 3400 cm^{-1}) and by the >90% reduction in relative intensity of the peaks between 1600 and 1800 cm^{-1} also reveals that most of the carbonyl groups present in the crude oil had been converted, either by loss as CO_2 or hydrogenation. From a GC-MS analysis of the crude bio-oil dissolved in either CHCl_3 or MeOH only a large peak of HOAc overlaying a broad undefined baseline rise with increasing temperature could be identified. Qualitatively, the upgrading reaction increases the number of volatile compounds as represented by multiple new peaks appearing at lower retention times in the GC traces of the product oil suggesting substantial changes in the composition of the oil to less reactive products and an overall lower average molecular weight and molecular weight distribution [38]. A series of peaks at lower retention times that were not present in trace of the crude oil could be assigned to low molecular weight alkenes and alkanes on the basis of their characteristic repetitive $\Delta m/z = 14$ ("CH₂") fragmentation pattern and by comparison to the retention times and fragmentation patterns of authentic samples. In addition, toluene could also be unambiguously identified as a product in the GC by direct comparison to an authentic sample. Thermogravimetric analysis (Fig. 3) shows an initial rapid loss of weight for the crude oil interpreted as loss of water by distillation to the inflection point at $\sim 125\text{ }^\circ\text{C}$ followed by slower further loss of water due to condensation reactions between 125 and $400\text{ }^\circ\text{C}$ and distillation of organic volatiles and a final residual weight of 5.5%. In contrast, the upgraded product oil gives a slower continuous weight loss leaving a final residue of 1.7 and 0.8% for the samples represented by entries 3 (top) and 5 (bottom) of **Table 2**, respectively.

Table 3 compares the results of the elemental and heating value analysis of the crude and the upgraded oil (corresponding to entry 3 of **Table 2**). Consistent with the micro-GC, IR and GC-MS results, a more than 10-fold decrease of the oxygen content (w/w) and a 3-fold increase of the energy density was achieved by the upgrading reaction. Further insights into the chemical composition changes of the same oil sample effected by the upgrading process were gained by the previously described chemical class separation protocol developed by Acikgoz and Kockar [32,39], which fractionates the oil by extraction with pentane with the insoluble residue denoted as *asphaltanes* followed by chromatographic separation of the pentane soluble extract on silica gel with n-pentane, toluene, and methanol as consecutive eluents of increasing polarity. Fig. 4 gives the results of this weight fraction analysis (WFA) after removal of the extraction solvent in vacuo showing a drop of the asphaltane content from $\sim 68\%$ to 3% (w/w), which is also reflected in the visual appearance of the oil (cf. Fig. 1). The stability of the crude vs the same upgraded oil sample was tracked by repeating the WFA after 30 and again 60 days. As Fig. 5 shows the crude oil shows an increase of pentane

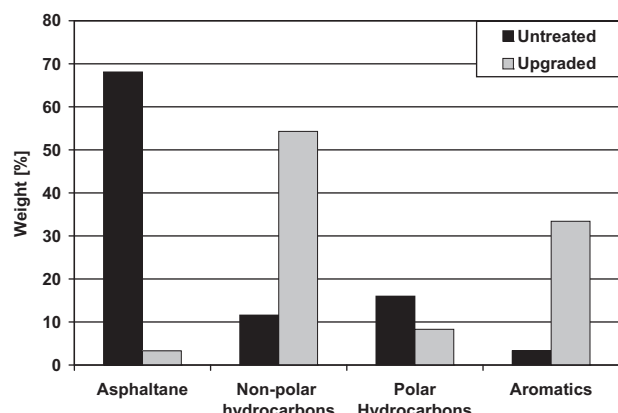


Fig. 4. Effect of the Red Mud catalyzed upgrading of the bio-oil (**Table 2**, entry 3) on the relative amounts of asphaltane, non-polar and polar hydrocarbons and aromatics, as gravimetrically determined by chemical class separation (weight fraction analysis) through chromatographic fractionation on an activated silica-gel column using n-pentane, toluene, and methanol as consecutive eluents.

insoluble asphaltanes to 92% over this period with a corresponding decrease in weight of the other fractions, while the composition of the upgraded oil remains almost constant. When repeated after storing the crude bio-oil in an airtight container at ambient temperature for more than 120 days the upgrading reaction failed, i.e., instead of a clear oil only a black sticky tar could be obtained, which is consistent with the results of the timed WFA (Fig. 5). The upgrading of the aged oil fails even if the reaction is pressurized with 5.52 MPa $\text{H}_2(\text{g})$ as an externally supplied reductant pointing to irreversible changes in the composition of the crude by the previously discussed condensation and re-oligomerization/re-polymerization reactions between the lignin derived phenol and aldehyde/ketone components of the oil [32].

3.3. Comparative before/after analysis of the Red Mud catalyst

As with the bio-oil a comprehensive before/after comparative analysis of the Red Mud (RM) used as the catalyst was carried out by a variety of techniques that give insights into its changes in composition during use with the highly acidic substrate. Visually, and as observed in our previous studies [32–34], the appearance of the catalyst changes from the brown-red of the virgin RM to gray, which immediately suggests a conversion of the hematite present into a different and likely reduced iron compound. Fig. 6 shows the appearance of the Red Mud before and after its use a

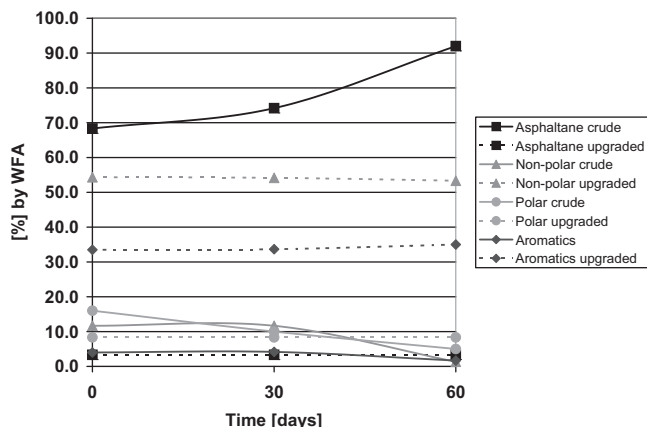


Fig. 5. Time evolution of the relative composition of the crude vs the upgraded bio-oil (**Table 2**, entry 3) by weight fraction analysis.



Fig. 6. Appearance of Red Mud before and after use as a bio-oil upgrading catalyst.

catalyst. The colour change is accompanied by a change in magnetic susceptibility, i.e., in contrast to virgin RM the transformed catalyst is attracted to magnets, e.g., it sticks to the magnetic stir bar used to agitate the reaction mixtures in the 316SS reactor. **Table 4** compares the results of magnetic susceptibility measurements of native RM vs the recovered gray material (in the following denoted as reduced Red Mud = RRM) against that of a 1% Fe_3O_4 standard in an inert matrix. The data shows a more than 10-fold increase on the magnetic susceptibility at both low and high frequency for the RRM vs RM. The percentage of frequency dependent susceptibility, which is a measure of the amount of ultrafine ($<0.03 \mu\text{m}$) superparamagnetic (SP) ferromagnetic particles present [40], decreases from RM to RRM, pointing to a sintering process in the catalyst during its use. Elemental analysis reveals a carbon content of $<0.1\%$ for virgin RM vs $\sim 33\%$ for the gray RRM, i.e., a substantial amount of the carbon supplied by the bio-oil is deposited into the RRM after a single use as a catalyst. This catalyst coking is consistent with the weight increase of the recovered catalyst given in the last column of **Table 2** and also the weight loss determined by Thermogravimetric Analysis (TGA) shown in **Fig. 7**, which amounts to $\sim 45\%$ by heating to 800°C in either air or N_2 atmosphere. The higher than 33% weight loss by TGA likely represents loss of crystal water bound in the matrix of the minerals present in the RM/RRM (cf.

Table 1), which is released at higher temperatures in addition to the weight of the carbon present. A sodicity analysis by ICP-MS shows the sodium content of virgin RM as 51.4 mg/g vs 28.9 mg/g for RRM. However, considering the weight added to the RRM by the carbon deposited the actual (w/w) sodicity remains essentially unchanged, which also suggests that very little sodium is leached into the organic product phase from the RM catalyst during its use [41].

The composition of RM and RRM before and after use as a catalyst was also analyzed by powder XRD (**Fig. 8**) and Mössbauer spectroscopy (**Fig. 9**). Sensitive only to the (micro-)crystalline phases of the material, a comparison of the XRD patterns before and after the reaction shows only small changes for the peaks of the Al, Si and Ti-based oxide minerals, but does indicate the formation of a new crystalline calcite (CaCO_3) phase, likely induced by the presence of abundant bio-oil derived CO_2 in the reaction mixture. More importantly, the XRD pattern reveals the appearance of the spinel ferrite maghemite ($\gamma\text{-Fe}_2\text{O}_3$), which is ferrimagnetic and possesses the same structure as magnetite, however with both the

Table 4

Magnetic susceptibility of the Red Mud before and after (reduced Red Mud) use as a catalyst vs a magnetite standard.

Sample	$\chi_{\text{LF}} \times 10^{-6} (\text{m}^3/\text{kg})$	$\chi_{\text{HF}} \times 10^{-6} (\text{m}^3/\text{kg})$	$\chi_{\text{fd}}\%$
Standard (1% Fe_3O_4)	1.375	1.329	3.35
Red mud	0.149	0.117	21.35
reduced Red Mud	2.02	1.94	3.94

With the following definitions

$$\kappa_{\text{corrected}} = \kappa_{\text{sample}} - (\text{first air-second air})/2$$

Mass specific susceptibility = κ/ρ

Percentage frequency dependent susceptibility = $(\chi_{\text{LF}} - \chi_{\text{HF}})/\chi_{\text{LF}} \times 100$

$$\chi_{\text{LF}} \text{ and } \chi_{\text{HF}}$$

$$\chi_{\text{LF}} \text{ and } \chi_{\text{HF}}$$

$$\chi_{\text{fd}}\%$$

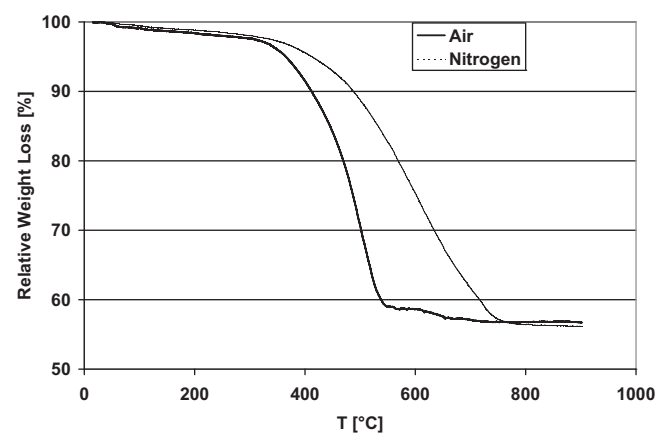


Fig. 7. Relative weight loss of reduced Red Mud in air and N_2 determined by thermogravimetric analysis (TGA).

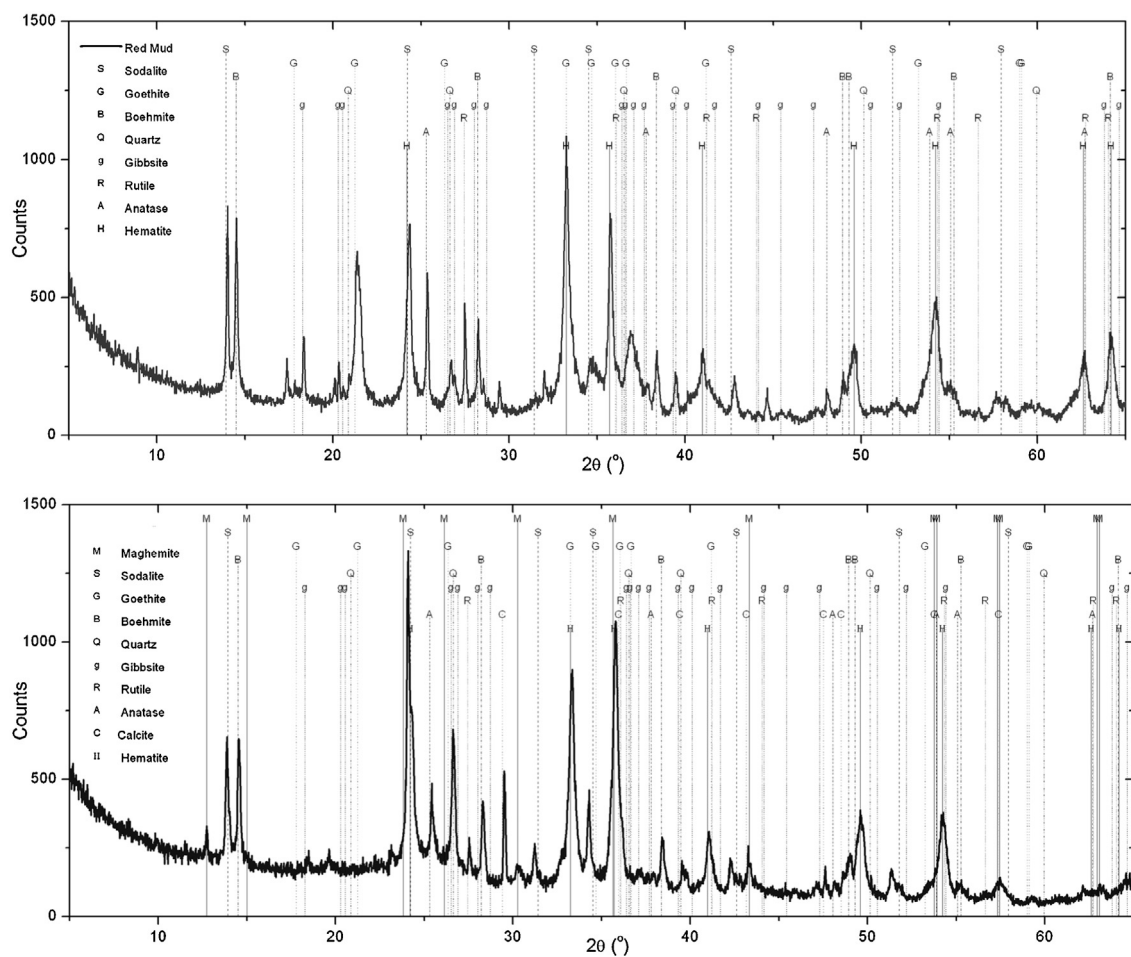


Fig. 8. Powder XRD patterns of Red Mud before (top) and after (bottom) its use as a catalyst (gray reduced Red Mud).

tetra- and octahedral position occupied by Fe^{III} cations. The Mössbauer analysis, which is also sensitive to amorphous iron mineral phases present, shows that ~50% of the hematite ($\alpha\text{-Fe}_2\text{O}_3$) has been converted to magnetite (Fe_3O_4), which, as it does not register in the XRD, must be present in a non-crystalline form. The conversion of hematite to either maghemite or magnetite, either by a phase transition and reduction (magnetite), or by phase transition and reduction followed by reoxidation (maghemite) explains

both the colour and magnetic susceptibility changes observed in conversion of RM to RRM.

Changes in the micro-structure of the RM are also observed by BET analysis (dinitrogen adsorption), which gives the low surface areas of $13.1 \pm 0.2 \text{ m}^2/\text{g}$ for RM and $6.0 \pm 0.1 \text{ m}^2/\text{g}$ for RRM [42]. As for the results of the magnetic susceptibility measurement discussed above, the lower surface area of the used catalyst RRM is also indicative of a sintering of the catalyst or be caused by the large amount of organic carbon being adsorbed by the RRM.

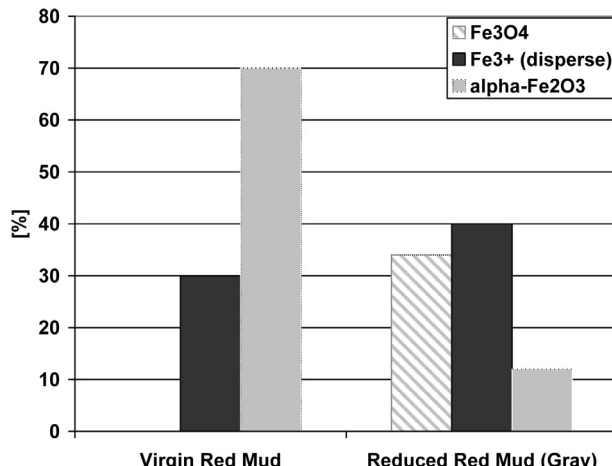


Fig. 9. Iron-oxide species in the Red Mud before (top) and after (bottom) its use as a catalyst (gray reduced Red Mud) as identified by Mössbauer spectroscopy.

4. Discussion

4.1. Bio-oil reactions

As explicitly formulated in our earlier reports [32,33,43], the observed deoxygenation of the bio-oil can in principle occur through loss of CO_2 (ketonization or direct decarboxylation) or loss of water (dehydration). The latter can either take place directly (forming esters, ethers and alkenes) or through iterative reaction cascades of initial hydrogenation of carbonyl groups to alcohols followed by renewed dehydration yielding alkenes, which in turn can then be hydrogenated to alkanes. The spectra in Fig. 2 (IR) and the micro-GC and GC-MS results (see Supplementary Material) provide direct evidence for this process taking place in the presence of the RM catalyst. As the pyrolysis bio-oil upgrading reactions described here proceed without the addition of an external reductant, the hydrogen required for the reduction steps must be derived from internal sources. Considering that ~33% of the weight

of the RRM is carbon, one major source is likely the breakdown of some of the bio-oil into CO_2 , hydrogen and coke, a process that has also been observed with Pt-based catalysts [44]. The presence of large amounts of CO_2 in the gas headspace of the reactions and the formation of a calcite phase in the RRM suggests that this does – along with ketonization of other carboxylic acids present in the oil – play an important role in the deoxygenation process. A further specific source of hydrogen could be the decomposition of formic acid believed to be present in the fresh bio-oil in substantial amounts. While our earlier work with RM demonstrated the viability of this pathway [33], we were not able to directly detect or quantify formic acid in the bio-oil. The quantitative determination of formic acid by GC in simple mixtures is in principle possible [45], however, for the bio-oil used here the complexity of the mixture and the need to use high GC injector temperatures of $T > 200^\circ\text{C}$ to mobilize the oil in the injector port prevented us from identifying or quantifying the actual amounts of formic acid present in the oil. Control experiments with authentic samples of formic acid in aqueous medium established its immediate decomposition in the injector port at these temperatures, i.e., no peaks for formic acid itself were observable in the GC traces.

4.2. Yields, mass balance and the role of water

At 24% (w/w for bio-oil used) the yield of liquid organic product (Entry 3, Table 2) isolated appears to be low. This evaluation must however be reflected against the almost three-fold increase in the heating value of the upgraded vs the crude oil. Given that the crude oil contains 43% oxygen by weight and an energy densification can only occur through substantial mass loss of oxygen as either water or CO_2 (a general and necessary feature of biomass deoxygenation) and the fact that an additional 2.4 g or 3.4 g (Entries 3 and 5, Table 2) of carbon are deposited into the catalyst matrix during the upgrading reactions, these low yields are not unexpected. The simultaneous changes in the oil, gas phase (formation of CO_2 and other volatiles) and catalyst composition, where the latter is also influenced by loss of weight by partial reduction from Fe_2O_3 to Fe_3O_4 and the formation of CaCO_3 (cf. Fig. 8) make an accurate determination of the overall carbon mass balance difficult. Using the values from entry 3, Table 2 and as an example and considering the elemental analysis results (Table 3), the approximate total amount of carbon in the organic product phase and the recovered catalyst is $5.9 \times 0.803 + (7 + 2.4) \times 0.33 = 7.8 \text{ g}$ compared to $25 \times 0.334 = 8.25 \text{ g}$, accounting for ~94% of the carbon in the bio-oil used with the balance then being contained in the gas phase and small amounts of polar water-soluble organics distributed into the aqueous product phase.

The positive effect of adding water to the reaction mixture appears counter-intuitive, but is chemically logical, as added water will suppress the formation of the undesired higher molecular weight products in the in equilibrium condensation, esterification, etherification and polymerization (by reversible hydration of alkenes) reactions. This is of particular importance when considering that the TGA data (Fig. 3) show substantial loss of weight (likely as water) at $T < 150^\circ\text{C}$, while the RM is not reduced to its catalytically active RRM form until temperatures $> 300^\circ\text{C}$ are reached [33,34]. Extensive cross-condensation reaction sequences can therefore take place in the mixture during the heating phase from ambient to the reaction temperature of 365°C . This also immediately suggests that the addition of water may not be necessary, if the heating rate of the oil is much more rapid, a scenario achievable by injecting the oil into a preheated catalyst bed in an ultimately preferable continuous flow process. If the only objective is the bio-oil upgrading reaction, an alternative approach would be to employ pre-reduced RM as the catalyst and/or reuse RRM, as

already successfully demonstrated in our study on the conversion of levulinic acid [34].

4.3. Limitations and challenges to using Red Mud as a catalyst: qualitative process viability assessment

When considered from a viewpoint of catalytic efficiency, obvious challenges and limitations to the use of RM as a upgrading catalyst arise from its overall low activity compared to, e.g., platinum group metals based systems such as Ru/C or Pt/ Al_2O_3 , and the fact that even with the extended reaction times employed in this initial study (4 h) the product oil retains residual acidity (pH 5–6, cf. Table 2). This residual acidity is likely associated with phenolic species originating from the lignin components of the hardwood used to produce the bio-oil, as it is unlikely that the Fe-based catalyst system is capable of hydrogenating aromatic rings to cycloalkanes, a transformation requiring much active catalysts systems [46]. However, we believe that the transformation of the Red Mud from a highly-alkaline hazardous waste with an associated substantial cost of initial disposal and unknown long-term environmental stewardship costs to an essentially non-toxic, carbon-enriched and in principle magnetically separable, non-alkaline material that may find use as an iron ore or at as a binder for the pelletization of iron ore, may offer substantial economic and ecological synergies that can offset its low catalytic activity. Two scenarios for the use of RM as a bio-oil upgrading catalyst emerge from this proposition:

In scenario 1, RM is shipped from a Bayer process or RM disposal site to a decentralized biomass processing facility producing pyrolysis bio-oil, where it is then used as a catalyst. In this scenario the RRM produced could be continuously reused. On the basis of our studies with levulinic acid [34], it can then be anticipated, that after the initial conversion of RM to RRM the catalytic activity would actually be enhanced and the upgraded oil yield improve, as no more carbon would be deposited into the catalyst matrix after the first use. Even though the RM can – due to its low cost, i.e., essentially the cost of its transportation to the processing site, preferably by barge or rail – be considered a *sacrificial* material, the overall objective in this scenario would be to maximize the bio-oil/RM ratio.

In scenario 2, bio-oil (or biomass with the pyrolysis carried out on-site) would be shipped to a Bayer process or RM disposal site and effectively used as *reagent* to convert the RM into the non-alkaline, less problematic and potentially value-added RRM. In this scenario the obvious objective would be to minimize the bio-oil/RM ratio and its implementation would require a careful life-cycle analysis and an economically and ecologically sustainable biomass feed taking into account the unique local parameters and logistics. If practiced on a large scale this scenario would possibly also allow a remediation of RM storage sites, as a variety of sodium tolerant plant covers are available, while to our knowledge no alkaline tolerant plants exists able to withstand the pH values imparted by RM [14]. A further modification of the second scenario would be the catalytic pyrolysis of biomass with RM being used as the heat carrier and catalyst, i.e., the direct co-processing of ligno-cellulosic biomass (rather than bio-oil) with Red Mud in which the pyrolysis and upgrading of the oil and the conversion of RM to RRM are combined in a single step.

Further studies aiming at optimizing the Red Mud catalyzed upgrading reaction of pyrolysis bio-oil as a function of the type of bio-oil used and reaction conditions employed (temperature, pressure, substrate/catalyst ratios and catalyst reuse) are currently under way in our laboratory as are experiments and engineering studies on the magnetic separability and concomitant iron oxide content enrichment of partially reduced Red Mud.

Acknowledgments

The authors thank Rio Tinto ALCAN (Jonquiere, Quebec Operation), for supplying an authentic operational process sample of Red Mud and funding for equipment and the Agricultural Biorefinery Innovation Network (ABIN) as funded by Agriculture and Food Canada, the Canada Brazil Network as funded by Kinross Gold and the CAPES program of the Brazilian Federal Government (scholarship to E.d.R.) for supporting this research.

Appendix A. Supplementary data

Supplementary data associated with this article can be found, in the online version, at <http://dx.doi.org/10.1016/j.apcatb.2013.02.007>.

References

- [1] S. Czernik, A.V. Bridgwater, *Energy & Fuels* 18 (2004) 590–598.
- [2] D. Mohan, C.U. Pittman, P.H. Steele, *Energy & Fuels* 20 (2006) 848–889.
- [3] D.A. Bulushev, J.R.H. Ross, *Catalysis Today* 171 (2011) 1–13.
- [4] A.V. Bridgwater, *Biomass and Bioenergy* 38 (2012) 68–94.
- [5] J.H. Marsman, J. Wildschut, F. Mahfud, H.J. Heeres, *Journal of Chromatography A* 1150 (2007) 21–27.
- [6] M. Garcia-Perez, A. Chaala, H. Pakdel, D. Kretschmer, C. Roy, *Biomass and Bioenergy* 31 (2007) 222–242.
- [7] P.M. Mortensen, J.D. Grunwaldt, P.A. Jensen, K.G. Knudsen, A.D. Jensen, *Applied Catalysis A* 407 (2011) 1–19.
- [8] A. Sanna, J.M. AndréSEN, *ChemSusChem* 5 (2012) 1944–1957.
- [9] It can be argued that Red Mud has in fact a negative value, as there are substantial costs associated with its disposal and storage as well as lost economic opportunity due to the failure to capture the intrinsic value of the iron and titanium ore contained in the material. The cost of Red Mud is therefore limited to the cost of safely transporting it to the site of its use.
- [10] See www.redmud.org for a general introduction and up-to-date overview and discussion.
- [11] G. Power, M. Grafe, C. Klauber, *Hydrometallurgy* 108 (2011) 33–45.
- [12] C. Klauber, M. Grafe, G. Power, *Hydrometallurgy* 108 (2011) 11–32.
- [13] M. Grafe, G. Power, C. Klauber, *Hydrometallurgy* 108 (2011) 60–79.
- [14] M. Grafe, C. Klauber, *Hydrometallurgy* 108 (2011) 46–59.
- [15] S. Everts, *Chemical and Engineering News* 88 (2010) 50–51.
- [16] S. Everts, *Chemical and Engineering News* 88 (2010) 11.
- [17] S. Everts, *Chemical & Engineering News* (2011), <http://dx.doi.org/10.1021/CEN012711144214>.
- [18] S. Everts, *Chemical and Engineering News* (2011), <http://dx.doi.org/10.1021/CEN010511102817>.
- [19] E.J. Grootendorst, R. Pestman, R.M. Koster, V. Ponec, *Journal of Catalysis* 148 (1994) 261–269.
- [20] R. Pestman, R.M. Koster, E. Boellaard, A.M. van der Kraan, V. Ponec, *Journal of Catalysis* 174 (1998) 142–152.
- [21] S. Sushil, V.S. Batra, *Applied Catalysis B* 81 (2008) 64–77.
- [22] S. Ordonez, *Applied Catalysis B* 84 (2008) 732–733.
- [23] M. Balakrishnan, V.S. Batra, J.S.J. Hargreaves, A. Monaghan, I.D. Pulford, J.L. Rico, S. Sushil, *Green Chemistry* 11 (2009) 42–47.
- [24] M. Balakrishnan, V.S. Batra, J.S.J. Hargreaves, I.D. Pulford, *Green Chemistry* 13 (2011) 16–24.
- [25] S. Sushil, V. Batra, *The Journal of Solid Waste Technology and Management* 37 (2011) 188–196.
- [26] S. Ordonez, H. Sastre, F.V. Diez, *Catalyst deactivation*, in: B. Delmon, G.F. Froment (Eds.), *Studies in Surface Science and Catalysis*, vol. 126, Elsevier Science Publ BV, Amsterdam, Netherlands, 1999, pp. 443–446.
- [27] S. Ordonez, H. Sastre, F.V. Diez, *Journal of Hazardous Materials* 81 (2001) 103–114.
- [28] S. Ordonez, H. Sastre, F.V. Diez, *Applied Catalysis B* 29 (2001) 263–273.
- [29] S. Ordonez, H. Sastre, F.V. Diez, *Applied Catalysis B* 34 (2001) 213–226.
- [30] S. Ordonez, F.V. Diez, H. Sastre, *Catalysis Today* 73 (2002) 325–331.
- [31] J.R. Paredes, S. Ordonez, A. Vega, F.V. Diez, *Applied Catalysis B: Environmental* 47 (2004) 37–45.
- [32] E. Karimi, C. Briens, F. Berruti, S. Moloodi, T. Tzanetakis, M.J. Thomson, M. Schlaf, *Energy & Fuels* 24 (2010) 6586–6600.
- [33] E. Karimi, A. Gomez, S.W. Kycia, M. Schlaf, *Energy & Fuels* 24 (2010) 2747–2757.
- [34] E. Karimi, E.D. Resende, C. Gissane, A. Gomez, S.W. Kycia, I.F. Teixeira, R.M. Lago, I. Aigner, C. Briens, F. Berruti, M. Schlaf, Preprint for the ACS Division of Fuel Chemistry – 242nd ACS Meeting, ACS Division of Fuel Chemistry, Denver, CO, 2011.
- [35] See Supplementary Material for a spec sheet as supplied by Rio Tinto ALCAN.
- [36] A digital image of this material is given in the Supporting Information.
- [37] See Fig. S1 in the Supplementary Material.
- [38] See Supporting Material (Figs. S2 and S3 for images of these GC-MS traces. The highly desirable identification of other components in the upgraded oil requires hi-res MS that was not yet available to us during this study, but will be attempted in future studies.
- [39] C. Acikgoz, O.M. Kockar, *Journal of Analytical and Applied Pyrolysis* 85 (2009) 151–154.
- [40] H.R. Owliaie, R.J. Heck, A. Abtahi, *Canadian Journal of Soil Science* 86 (2006) 97–107.
- [41] This is not necessarily true for the aqueous phase also generated. A complete tracking of sodium contents of the liquid product phases will be carried out in future larger scale process optimization studies.
- [42] The isotherms and multi-point BET plots for these measurements are given in the Supplementary Material. The original data sheet for the RM as supplied by Rio Tinto ALCAN specifies a surface area of 10–40 m²/g.
- [43] E. Karimi, I.F. Teixeira, L.P. Ribeiro, A. Gomez, R.M. Lago, G. Penner, S.W. Kycia, M. Schlaf, *Catalysis Today* 190 (2012) 73–88.
- [44] C.A. Fisk, T. Morgan, Y.Y. Ji, M. Crocker, C. Crofcheck, S.A. Lewis, *Applied Catalysis A* 358 (2009) 150–156.
- [45] See e.g. Agilent Technologies Application Brief 5990-4456EN, <http://www.chem.agilent.com/Library/applications/5990-4456EN.pdf>
- [46] H. Ohta, H. Kobayashi, K. Hara, A. Fukuoka, *Chemical Communications* 47 (2011) 12209–12211.